

Picosecond optical nonlinearity in monolayer-protected gold, silver, and gold-silver alloy nanoclusters

Reji Philip* and G. Ravindra Kumar

Tata Institute of Fundamental Research, Homi Bhabha Road, Colaba, Bombay-400005, India

N. Sandhyarani and T. Pradeep

Department of Chemistry and Regional Sophisticated Instrumentation Centre, Indian Institute of Technology, Madras 600 036, India

(Received 20 December 1999; revised manuscript received 19 May 2000)

Monolayer-protected Au, Ag, and Au:Ag alloy nanoclusters have been synthesized using octanethiol and octadecanethiol as capping agents. The particle-size distribution is narrow with an average core size of 3–4 nm. Optical nonlinearity induced by 35 ps pulses at 532 nm has been investigated in these samples using the Z-scan technique. It is found that in general, they behave either as saturable absorbers or reverse saturable absorbers depending on the intensity of excitation. Au and Ag clusters show nearly the same efficiency for optical limiting, but the alloy clusters are found to be less efficient in limiting and are less photostable. The observed effects are explained in terms of the electron dynamics of the excited-state species.

INTRODUCTION

Intense research is currently being pursued in the field of nanoparticles by various laboratories, motivated by the fundamental question of how material properties evolve with increasing size in this intermediate region between the molecular and the bulk regimes. On the application side, nanoparticles are expected to lead to a vista of modern materials for the miniaturization of electronic devices.^{1–5} Other possible future applications include ultrafast data communication and optical data storage.^{3–5} Oriented pearl-necklace arrays of metallic nanoparticles in polymers are suggesting routes to polarization-dependent color filters, to be used in liquid crystal displays (LCD's).⁶ Metal nanoparticles have found important applications as catalysts because of their high surface-to-volume ratios,⁵ and semiconductor nanoparticles are being used in the fabrication of solar cells.⁷

Metal nanoparticles possess interesting optical properties. For example, nanoparticles of alkali metals and noble metals copper, silver and gold show a broad absorption band in the visible region of the electromagnetic spectrum,^{8,9} which is substantially different from the flat absorption of the corresponding bulk metal in this region. The origin of this absorption band is attributed to the electromagnetic field-induced collective oscillation of the free conduction electrons occupying states near the Fermi level in the conduction band (surface plasmons).² It is shown that the plasmon absorption band characteristics can be changed by altering the nanoparticle size and shape.¹⁰ Furthermore, composite colloids and alloys can be formed from nanoparticles of different metals, whereby the physical properties can be selectively controlled over a larger range. This synthetic flexibility of the physical and chemical properties is one of the reasons why metal nanoparticles are interesting candidates for nonlinear optical applications like optical limiting. Applications of optical limiters include sensor and eye protection,¹¹ optical communications,¹² and optical information processing.¹³ They represent a class of optical bistable materials¹⁴ which have been demonstrated to be useful for optical computing

functions like logic gating and pattern recognition.¹⁵

These facts have accelerated the progress in the synthetic techniques for stable nanoparticles, and it has been shown that nanosized metal clusters can be prepared and stabilized using thiols as capping agents.¹⁶ Recently, we synthesized and characterized monolayer-protected clusters (MPC's) of Au and Ag and monolayer-protected alloy clusters (MPAC's) Au:Ag using octanethiol (OT) and octadecanethiol (ODT) as capping agents, as per a modified literature procedure.^{17,18} All these clusters have been characterized by different techniques such as TEM, XRD, IR, DSC, TGA, XPS, Mass, NMR, and absorption spectroscopy.^{17,18} The transmission electron micrograph image obtained for the ODT capped Au cluster (designated as AuODT) is shown in Fig. 1 (Inset I shows the schematic of such a cluster with a truncated octahedron morphology). The particle-size distribution is nearly homogeneous with an average size of 3.0 ± 0.5 nm. Ag clusters are found to have a larger core diameter of 4.0 ± 0.5 nm (micrograph not shown). Core size is seen to be largely independent of the capping molecule in both Au and Ag clusters, in the synthetic conditions used. UV/VIS absorption spectra of the clusters dissolved in toluene are shown in inset II of Fig. 1. The peak maximum corresponding to the plasmon excitation occurs around 520 nm in Au clusters, and 450 nm in Ag clusters. In addition, we observed the same peak maxima in all the clusters independent of the chain length. The only difference between the spectra is the width of the peaks, which is found to increase with chain length.¹⁷ The alloy clusters which are stabilized with ODT have an average size of 3.0 ± 0.5 nm and their peak maxima fall in-between that of Au and Ag clusters. As the Au composition increases, the peak undergoes a red shift as expected.¹⁹ This spectral behavior rules out any substantial formation of monometal MPC's and core-shell structures.²⁰

In this paper we report the picosecond optical nonlinearity of these compounds measured using the z-scan²¹ technique. It is seen that at moderate pump intensities these samples exhibit a saturable absorber behavior, whereas all samples

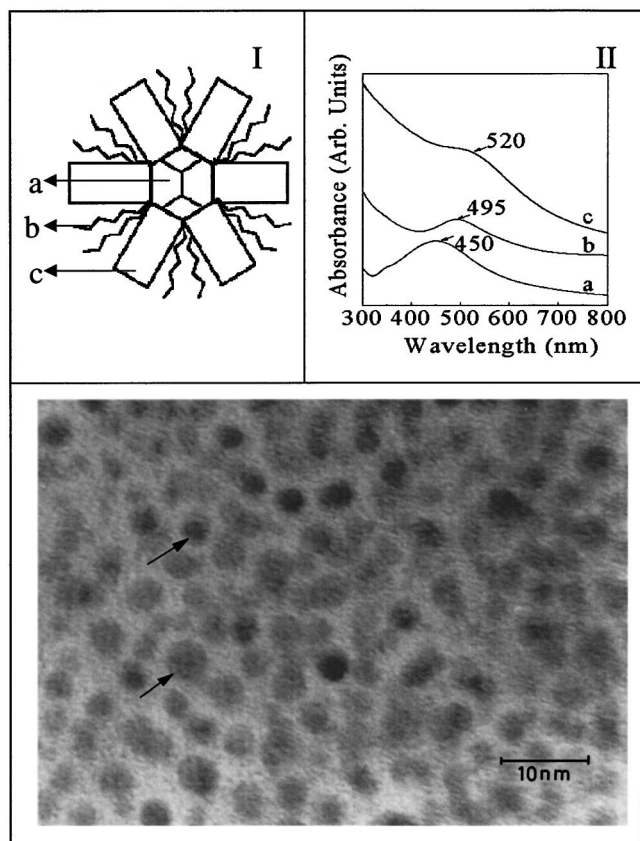


FIG. 1. Transmission electron micrograph of AuODT. Lattice images are marked with arrows. Inset I shows the schematic of a cluster. (a), (b), and (c) represent cluster core, unorganized alkyl chains, and ordered alkyl chains, respectively. Inset II shows the absorption spectra of (a) AgODT and (b) AuAg_{0.33} and (c) AuODT clusters. Plasmon excitation peaks are marked.

show strong optical limiting at still higher intensities. The electron dynamics responsible for this peculiar nonlinear behavior in these systems is discussed.

EXPERIMENTAL

Details of sample synthesis have been discussed elsewhere.¹⁷ In short, Ag⁺ (or Au³⁺) ions are phase transferred to the toluene phase (from the aqueous medium) by a phase transfer reagent. To the resulting mixture, the thiol solution in toluene is added with vigorous stirring. The metal ions are reduced subsequently by the slow addition of aqueous sodium borohydride solution. The solution of the clusters is stirred overnight and the organic layer is separated. The clusters are precipitated by adding methanol and the resulting powder is washed several times with methanol to remove impurities and is air dried. Monolayer-protected Au:Ag alloy clusters also have been synthesized by the same method, by starting with mixtures of Ag⁺ and Au³⁺ with appropriate stoichiometry. For measurements discussed here we used compositions corresponding to AuAg_{0.75}, AuAg_{0.67}, and AuAg_{0.33}. All these clusters are soluble in nonpolar solvents.

Briefly, in a typical *z*-scan experimental setup, a laser beam with a transverse Gaussian profile is initially focused by a lens. The sample, the thickness of which is kept less than half the confocal length, is then moved along the axial

direction of the focused beam in such a way that it moves away from the lens, passing through the focal point. At the focal point the sample experiences the maximum pump intensity, which will progressively decrease in either direction of motion from the focus. If a light detector is placed in the far field and the transmitted intensity is measured as a function of the position of the sample, one obtains an “open aperture” *z*-scan curve, the shape of which will reveal the presence of any absorptive nonlinearity in the sample. On the other hand, if a properly chosen aperture is placed in front of the detector, a “closed aperture” *z*-scan curve is obtained which will reflect the occurrence of refractive nonlinearities.

For our *z*-scan experiments, neat solutions of the samples are prepared by dissolving them in toluene, centrifuging for five minutes and collecting the supernatant liquid. Sample concentrations are so adjusted that every sample has a linear transmission of 50% at the excitation wavelength for a 1 mm pathlength. Solutions taken in a 1 mm quartz cuvette are excited by 532 nm, 35 ps plane polarized pulses from the second harmonic output of a hybrid mode-locked Nd:YAG laser. The laser operates at a 10 Hz repetition rate. The pulses are spatially and temporally Gaussian, and the beam diameter is approximately 0.8 cm. The beam spot radius at the focal point is measured to be approximately 14 microns. The cuvette is fixed on a microprocessor controlled translation stage that has a range of 30 cm and a resolution of 2 microns, so that it can be accurately moved through the focal region of the laser beam. A fast photodiode monitors the input laser energy, and an energy meter collects the transmitted beam. For the closed aperture measurements, a suitable aperture is placed in front of the energy meter. Data acquisition is facilitated in real time by the use of a PC.

The optical limiting data have been extracted from the open aperture *z*-scan measurements. From separate measurements we have found that the solvent toluene also shows an absorptive nonlinearity at the intensities used. The samples show both absorptive and refractive nonlinearities.

The *z*-scan setup has been tested by measuring the third order nonlinear refractive index intensity coefficient γ of the standard sample CS₂. An average value of 1.7×10^{-11} esu was obtained, in good agreement with the reported value of 1.2×10^{-11} esu.²¹

RESULTS

In a typical open aperture *z* scan, the open aperture transmission normalized to the linear transmission of the sample is plotted against the sample position measured relative to the beam focus. Nonlinear absorption will be indicated by a smooth valley-shaped curve, symmetric about the focal (*z* = 0) position. Curiously, in the open aperture *z* scans obtained from the present samples we have seen unusual “humps” flanking the valley, as shown in Fig. 2 for an AuOT solution. These humps appear in varying strengths for the samples studied, and as will be discussed later, we believe that they arise from the bleaching of the ground-state plasmon band prior to free-carrier absorption. Figure 3(a) depicts the nonlinear transmission plotted as a function of the input laser fluence for toluene solutions of OT and ODT capped Ag nanoclusters. The nonlinear transmission of toluene due to two-photon absorption is well known,²² and the

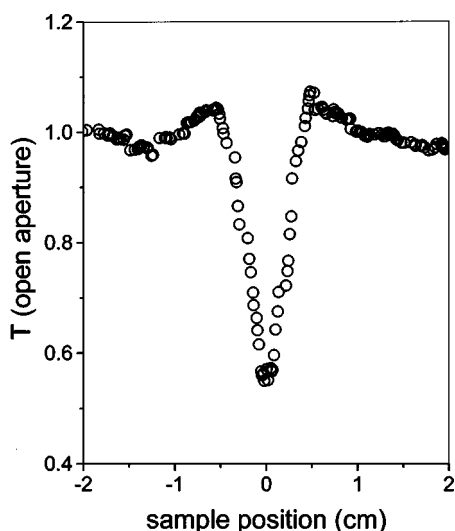


FIG. 2. A typical open aperture z scan (shown here for AuOT dissolved in toluene) obtained for the metal nanoclusters investigated. The “humps” seen flanking the valley arise from the bleaching of the ground-state plasmon band.

nonlinearity we observed for pure toluene is shown in the figures (“transmittance” here is identical to the normalized open aperture transmission). It is obvious from the figure that

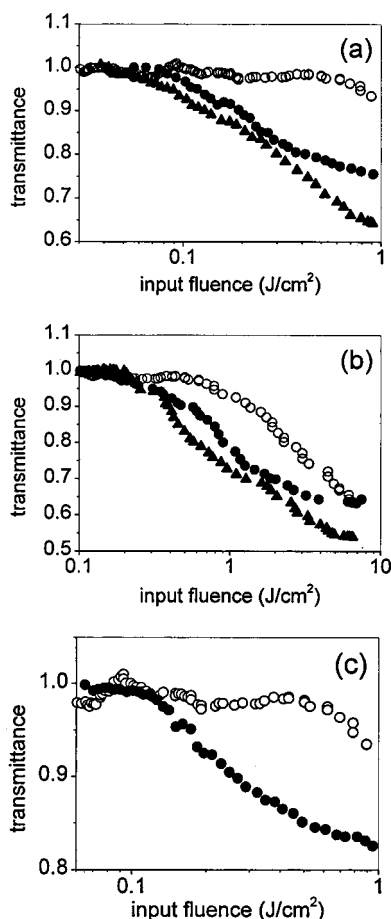


FIG. 3. Optical limiting in the clusters (a) Ag, (b) Au, and (c) AuAg_{0.75}, dissolved in toluene. Open circles show limiting in pure toluene. Solid circles are for ODT capped clusters while triangles are for OT capped clusters.

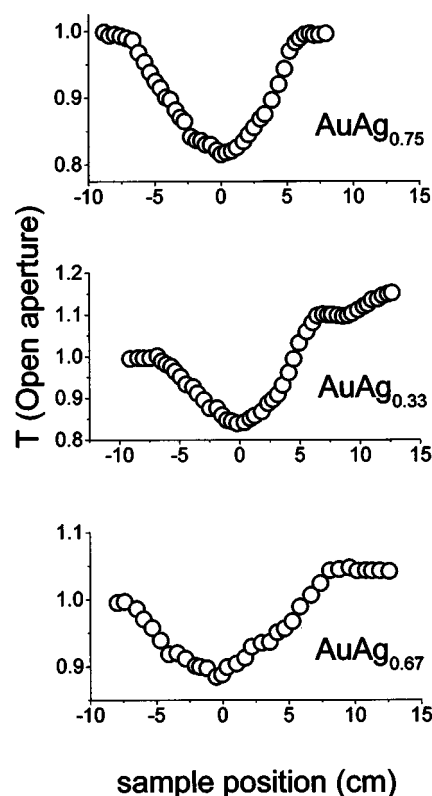


FIG. 4. Open aperture z scans of the three MPAC samples, AuAg_{0.75}, AuAg_{0.33}, and AuAg_{0.67}, dissolved in toluene. In the actual experimental setup, scans start at the negative z side and end at the positive z side. For AuAg_{0.33} and AuAg_{0.67} the net transmission has increased after laser irradiation, indicating that photodamage has occurred.

octanethiol capped clusters show a better limiting than octadecanethiol capped clusters. Similarly, Fig. 3(b) shows the limiting behavior of AuOT and AuODT (here the input laser fluence range has been extended to 10 J cm^{-2}), and the former is again found to have a better limiting efficiency. Furthermore, in both cases the ODT samples show a tendency for saturation of limiting at higher fluences, whereas such a trend is not equally obvious for the OT samples. A careful comparison of Figs. 3(a) and 3(b) shows that the limiting capability of Ag nanoclusters is somewhat better than that of the Au nanoclusters by virtue of their early onset of limiting and larger reduction in transmittance. The onset of limiting occurs around an input fluence of 0.1 J cm^{-2} ; this value compares favorably with that observed in polymer-stabilized nanocrystalline Ag and Ag₂S particles under nano-second excitation.²³

To investigate the effect of MPAC composition on the nonlinearity, we carried out measurements on the limiting behavior of Au:Ag alloy nanoclusters prepared with different Ag mole fractions of 0.33, 0.67, and 0.75, respectively. Figure 3(c) shows the results obtained for AuAg_{0.75}, the cluster containing the highest mole fraction of Ag. In terms of the reduction in transmission achieved, the limiting efficiency is found to be less as compared to the pure Au or Ag clusters. The open aperture z scans obtained for the three MPAC samples are shown in Fig. 4. Asymmetric curves have been obtained for AuAg_{0.67} and AuAg_{0.33}, which indicate probable photofragmentation of these two clusters at the laser intensities used.

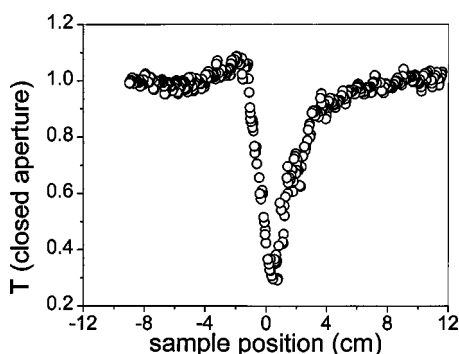


FIG. 5. Closed aperture z scan of AuOT dissolved in toluene.

Figure 5 shows a typical closed aperture z scan, obtained for AuOT in toluene. The peak-valley structure of the curve is a clear indication of a negative refractive nonlinearity exhibited by the medium.²¹ All samples have given the same kind of closed aperture z scans.

DISCUSSION

As noted before, the plasmon band of metal nanoclusters arises from the oscillations of the free electrons in the conduction band which occupy energy states near the Fermi level. Mie theory,²⁴ and its modified form, Maxwell-Garnett theory,^{2,8,9} have considered the effects of particle size on the plasmon band. These theories have predicted and it has been experimentally confirmed that the peak position shifts to the red and the band broadens as the size of the nanoparticles increases. However, it is the curious fact that the surface plasmon band is sensitive to laser excitation that makes metal nanoclusters particularly suitable for nonlinear optical applications. For example, recent investigations have shown that strong, broadband transient absorption occurs in gold²⁵ and silver²⁶ nanoclusters on a subpicosecond time scale when excited with a uv or visible laser pulse. The excited electron ("hot" electron) dynamics has been probed in detail for gold,²⁵ silver,²⁶ and gold-silver alloy²⁷ nanoclusters. The same has been investigated also by picosecond transient grating spectroscopy²⁸ and femtosecond transient absorption spectroscopy.²⁹ A general understanding as to the dynamics of electron relaxation in excited metal nanoparticles has been arrived at as a result of these investigations.

In brief, a laser pulse can cause an interband or intraband electron transition in the metal nanoparticle system, depending on the excitation wavelength and intensity. The electrons thus excited are free carriers possessing a whole spectrum of energies, both kinetic and potential, immediately after the absorption. The potential energies are those of the formerly unoccupied and occupied states within the conduction band. This excitation leads to a bleach, or reduction in intensity, of the ground-state plasmon band that is almost synchronous with the primary photon absorption (which occurs at the "zero time"). However, this process is also accompanied by the nascent excited state showing a transient absorption spectrum that is considerably broadened due to the nature of free-carrier absorption. Now the hot electrons will exchange energy with each other to form an "internally thermalized distribution." It is shown that this electron-electron coupling

occurs within 600 fs for thin gold films³⁰ and 500 fs for 15 nm gold nanoparticles.²⁷ After electron thermalization and partly during that process, electrons lose their energy further by externally thermalizing with the lattice. This process occurs through electron-phonon interactions, which has been studied extensively for bulk metals.³¹ The thermalization time for the electronic gas through electron-phonon coupling is measured to be 2–3 ps for bulk gold,³² and an almost identical time of 2.5 ps has been obtained for 15 nm gold nanoparticles.²⁵ This electron thermalization with the lattice is synchronous with a substantial recovery of the ground-state plasmon absorption band, so that the fast phase of the transient absorption scenario is over within a few picoseconds from the point of laser excitation.

Because of the phonon-phonon relaxation processes that follow, thermal energy will be dumped into the solvent causing the dielectric or surrounding medium to change, thereby influencing the plasmon resonance frequency of the nanoclusters. The result is that the full recovery of the ground-state plasmon band is delayed further. Kamat *et al.*²⁶ reports the lifetime of this slow component to be ~ 90 ps for 40–60 nm diameter silver colloids. Ahmadi *et al.*²⁵ found a lifetime of >50 ps for the lattice phonons in 15 nm gold nanoparticles, which is also in agreement with the results of the nonlinear optical studies of gold nanoparticles by Heilweil and Hochstrasser.²⁸ Thus, the broadband transient absorption that gains control at zero time subsides within about 100 ps giving way to the complete recovery of the bleached spectrum.

In addition to transient absorption, the possibility of photoejection of electrons also should be considered as a contributing factor leading to optical limiting in nanoclusters. This is an ultrafast phenomenon, which usually occurs by a two-photon or multiphoton absorption process,²⁶ since the pump-laser photons in the visible spectral region are usually not energetic enough for monophotonic electron ejection. Because of the lower density of states in the conduction band of metal nanoparticles, photoemission of electrons into the solvents can be significantly enhanced compared to that in the bulk material. Some of the ejected electrons undergo quick recombination, but the rest will accumulate at or near the cluster surface charging them electrically. This in turn causes them to disintegrate and form smaller size particles, particularly if the clusters are large in size. Additional confirmation to such photofragmentation of clusters has been obtained from TEM images and post-excitation absorption spectra.²⁶ (It may be noted here that thiol capped clusters are rather stable. The Au-S bond energy is of the order of 100 kcal/mol (Ref. 33) and monolayer desorption starts only around 270 °C,¹⁷ which means that the monolayers protect the clusters fairly well. Nevertheless, photofragmentation of the core does not necessarily get inhibited by the presence of monolayers). From transient absorption studies in Ag nanoclusters, Kamat *et al.*²⁶ have proposed the existence of a transient state Ag^+e^- that exists before fragmentation. This is essentially an aggregate of smaller clusters and trapped electrons distributed close to each other, which is generated in a photoinduced intraparticle charge separation process. They have observed that a supplementary long-lived (peaking in 1.5 ns), broad absorption in the visible and infrared wavelengths is being exhibited by the excited Ag nanoclus-

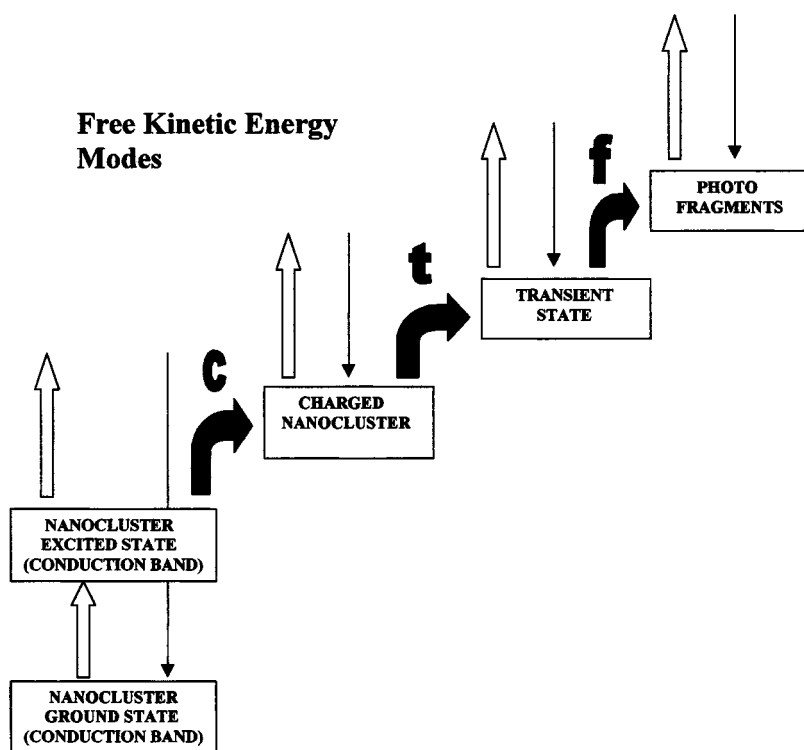


FIG. 6. Electron dynamics in the metal nanoclusters. Upward arrows represent plasmon absorption or free-carrier absorption, as applicable (see text). Downward arrows represent electron-phonon relaxation. *c*: multiphoton-induced electron ejection (ultrafast), *t*: transient state formation (\sim nanoseconds), and *f*: fragmentation.

ters, which they assign to this intermediate state (it is well known that aggregation of small Ag particles leads to a broad plasmon absorption band across the entire visible spectrum²). Its time constant of 1.5 ns gives the time frame with which chemical and physical changes occur in the parent Ag cluster following the photoejection of electrons to form the transient intermediate. Similar photoinduced redox processes have been proposed to be responsible for the optical limiting of 532/355 nm 30 ps laser pulses in AgBr nanosols also, which were comprised of 60 Å particles.³⁴

It is possible to explain the optical nonlinearity exhibited by the present metal nanoclusters on the basis of their rather complex excited-state dynamics discussed so far. From the femtosecond transient absorption studies conducted by Link *et al.*,²⁷ we note that the general mechanisms and timescales for electron cooling in Au:Ag alloy nanoclusters are essentially similar to those in pure Au and Ag nanoclusters. In particular, we have realized in the course of these experiments that metal nanoclusters belong to a group of materials where saturable absorption³⁵ (SA) and reverse saturable absorption³⁶ (RSA) happen at the same pump wavelength for different pump intensities. Here the mechanism is as follows: the bleach of the ground-state plasmon band occurring at moderate intensities is an SA process that results in an increase of optical transmission; on the other hand, the transient absorption (caused by free carriers) which becomes significant for increased pump intensities is phenomenologically similar to an RSA process leading to a reduced transmission. Numerical simulations of a reverse process, i.e., the changeover of a nonlinear absorber from an RSA regime to an SA regime for increased pump intensities, have been carried out earlier by Hughes and Wherret,³⁷ and Deng *et al.*³⁸ The circumstance for these studies is the fact that at very high intensities even the excited-state absorption that causes RSA can saturate, thus limiting the dynamic range of the optical limiter. Such behavior has been demonstrated ex-

perimentally also, by exciting the laser dye HITCI (1,1',3,3',3',3'-hexamethylindotricarbocyanine iodide) at 532 nm far away from its absorption peak of 740 nm.³⁹ However in the present case, the change is from an SA to RSA regime for our samples, since they are excited close to their absorption peaks. Within the pump intensities employed, we did not see a further change-over to the SA regime. It may also be mentioned here that media exhibiting intensity-dependent SA and RSA at the same wavelength have interesting other applications like efficient laser pulse narrowing⁴⁰ as well.

In this context, the advantage of a z -scan measurement is that it can separate the intensity dependent SA and RSA "spatially," as becomes evident from Fig. 2. When the sample is far away from the focal point, the pump intensity is too weak to induce any nonlinearity and the transmittance is equal to unity. As the sample is moved further towards the focus the intensity is increased so that ground-state plasmon bleach (resulting in SA) occurs; hence more light is transmitted and the transmittance becomes higher than unity. Still higher pump intensities will be seen by the sample as it nears the $z=0$ position (focal point), and free carrier absorption dominates in this region (resulting in RSA) causing limiting; hence less light is transmitted and the transmittance falls drastically to values less than unity. The increase in transmittance from unity followed by a decrease will make a local "hump" in the curve, as seen in the present case.

In view of these, a scheme for electron dynamics as presented in Fig. 6 can be considered. Picosecond laser excitation of the present thiol capped Ag, Au and alloy nanoclusters at 532 nm results in an intraband electron excitation within the conduction band, leading to a ground-state plasmon bleach. This is accompanied by broadband transient absorption by the free carriers in a subpicosecond time scale. In addition, there is the possibility that multiphoton induced electron ejection will generate electron-hole pairs in the nanoparticle structure, resulting in strong free-carrier absorp-

tion again in the subpicosecond time domain. Both the above mechanisms should contribute to the nonlinear absorption exhibited by these samples. The consistently enhanced limiting efficiency of octanethiol capped nanoclusters which is evident from Figs. 2 and 3 reveals that the capping material also plays a role in determining the optical nonlinearity of the nanocluster system. Presently the exact role of the ligand monolayer is not very clear: it may be that its presence actually modifies the nonlinearity of the cluster core; it is also possible that it is only passively adding its own nonlinearity to that of the core material. Figure 3(c) shows limiting in the alloy nanocluster $\text{AuAg}_{0.75}$ which is found to be not so efficient as in the pure metal clusters. It may be noted here that in general, ligand protected alloy clusters are thermally more stable than their monometal counterparts, but however, the presence and proportion of certain metals will enhance stability (e.g., Ag) while others cause instability (e.g., Cu).⁴¹ In view of this, our open aperture z -scan results shown in Fig. 4 are an indication towards the photostability of Au:Ag MPAC's. $\text{AuAg}_{0.75}$ gives a symmetric curve about the focal position showing proper recovery of the linear transmission after experiencing intense irradiation at the beam focus. However, the other two samples ($\text{AuAg}_{0.67}$ and $\text{AuAg}_{0.33}$) give unsymmetric curves indicating that their net transmission actually increases after laser irradiation, which is an obvious signature of photochemical change. Moreover, this increase is a maximum in $\text{AuAg}_{0.33}$, which is the sample containing the minimum Ag mole fraction in the present lot of samples. All samples have been irradiated by 60 mJ, 35 ps laser pulses at a 10 Hz repetition rate for about four minutes. This result proves that although the pure metal Au and Ag nanoclusters are quite photostable, in the MPAC form the stability of Au:Ag depends on the Ag mole fraction. We believe that as compared to the monometal clusters, electron ejection and subsequent photofragmentation occurs more strongly in the MPAC's probably leading even to cluster dissolution. It is possible that the MPAC stability is related to the spatial distribution of the metals in the cluster core. MPAC's are in general partially surface segregated in structure, and the more nobler metals tend to prefer nonsurface sites.⁴² For example, in an $\text{AuAg}_{0.4}$ MPAC core, approximately 60% of the surface sites were found to be occupied by Ag atoms.⁴¹ The question of whether it is possible to lay out the constituent metals in an MPAC in a chosen pattern over the core surface, and whether better stabilities can be achieved in this way, can perhaps open a number of interesting synthetic possibilities. The samples also display a negative refractive nonlinearity revealed by their peak-valley type closed aperture z scans as shown in Fig. 5. This is a direct consequence of the electron-phonon relaxation in the medium, which is a nonradiative process. The immediate vicinity of the irradiated volume is heated up leading to a reduction in the local refractive index, resulting in the self-defocusing of the beam.

It is appropriate to mention here that free-carrier absorption in Ag is considered to be the cause for strong nanosecond optical limiting found in $\text{Ag}_2\text{S}/\text{CdS}$ nanocomposites of 10 nm diameter,⁴³ and polymer-protected nanocrystalline Ag metal and Ag_2S particles of 6 nm diameter.²³ There are other reports also, where the optical limiting thresholds for silver containing metal-halide clusters and nanosols are found to be

substantially lower than those of the benchmark materials fullerenes and metallophthalocyanines.^{11,34} Our studies reveal that under picosecond laser excitation monolayer protected gold nanoclusters show an optical limiting efficiency that is of the same order as their silver counterparts. Results obtained from our recent nanosecond excitation studies⁴⁴ also lead to the same conclusion, and in addition, the optical limiting efficiencies are found to be higher in this case, as can be expected for RSA materials. In any case, a significant advantage of nanoclusters over conventional limiters is that the transient absorption spectrum is much broader and the process is an ultrafast phenomenon. This time factor has a particular significance: for those organic and organometallic limiters depending on triplet-triplet absorption, the intersystem crossing time can be as large as hundreds of picoseconds, thereby restricting the efficient application of their RSA to the limiting of comparatively longer (nanosecond and subnanosecond) laser pulses. On the other hand, with their broadband transient absorption manifest in femtosecond timescales, properly engineered nanoclusters can be expected to become the generation optical limiters developed for femtosecond laser pulses in the future.

CONCLUSION

Picosecond optical nonlinearity in octanethiol and octadecanethiol capped gold, silver and gold-silver alloy nanoclusters has been investigated by the z -scan technique. At comparatively lower pump intensities the ground-state plasmon bleach leads to a saturated absorption, and at higher intensities strong optical limiting is observed due to free-carrier absorption. The limiting efficiency is found to be of the same order in both Au and Ag clusters. Their photostability is found to be good. It is observed that octanethiol capping yields a better limiting as compared to octadecanethiol capping in both media. A comparatively weaker limiting is observed in the Au:Ag alloy nanoclusters, and it is found that the stoichiometry of the Au:Ag MPAC affects its photostability. Results indicate that among alloy clusters those with a higher Ag mole fraction are more photostable. The free-carrier absorption being broadband in nature and almost synchronous with the primary absorption, metal nanoclusters have tremendous potential to be developed into a class of ultrafast, broadband optical limiters. Furthermore, since the bleach recovery of the ground-state plasmon band is generally in the order of picoseconds, they can also be used as fast optical switches.

ACKNOWLEDGMENTS

The authors thank Vinod Kumarappan and M. Krishnamoorthy for writing the data acquisition software. R.P. wishes to thank the management of Sacred Heart College, Thevara, Cochin for the grant of a post-doctoral study leave. T.P. acknowledges financial support from the Department of Science and Technology, Government of India, for supporting his research program on monolayers. N.S. acknowledges financial support from the Council of Scientific and Industrial Research.

- *Present address: Raman Research Institute, Bangalore 560 080, India
- ¹A. P. Alivisatos, *J. Phys. Chem.* **100**, 13 226 (1996).
- ²U. Kreibig and M. Vollmer, *Optical Properties of Metal Clusters* (Springer, Berlin, 1995).
- ³A. S. Edelstein and R. C. Cammarata, *Nanoparticles: Synthesis, Properties, and Applications* (Institute of Physics Publishing, Bristol, 1996).
- ⁴P. V. Kamat and D. Meisel, *Studies in Surface Science and Catalysis*, Vol. 103, *Semiconductor Nanoclusters-Physical, Chemical and Catalytic Aspects* (Elsevier, Amsterdam, 1997).
- ⁵G. Schmid, *Clusters and Colloids: From Theory to Application* (VCH, Weinheim, 1994).
- ⁶Y. Dirix, C. Bastiaansen, W. Caseri, and P. Smith, *Adv. Mater.* **11**, 223 (1999).
- ⁷M. Graetzel, in *Electrochemistry in Colloids and Dispersions*, edited by R. A. Mackay and J. Texter (VCH, Weinheim, 1992).
- ⁸C. F. Bohren and D. R. Huffman, *Absorption and Scattering of Light by Small Particles* (Wiley, New York, 1983).
- ⁹M. Kerker, *The Scattering of Light and Other Electromagnetic Radiation* (Academic, New York, 1969).
- ¹⁰S. Link and M. A. El-Sayed, *J. Phys. Chem. B* **103**, 4212 (1999), and references therein.
- ¹¹S. Shi, W. Ji, S. H. Tang, J. P. Lang, and X. Q. Xin, *J. Am. Chem. Soc.* **116**, 3615 (1994).
- ¹²D. M. Russ, *Proc. SPIE* **630**, 161 (1986), and references therein.
- ¹³S. Laval, *Proc.-Electrochem. Soc.* **93-10**, 3 (1992).
- ¹⁴H. M. Gibbs, *Optical Bistability-Controlling Light with Light* (Academic, New York, 1985).
- ¹⁵S. W. Koch, N. Peyghambarian, and H. M. Gibbs, *J. Appl. Phys.* **63**, R1 (1988).
- ¹⁶M. J. Hosteller and R. W. Murray, *Curr. Opin. Colloid Interface Sci.* **2**, 42 (1997).
- ¹⁷N. Sandhyarani, M. R. Resmi, R. Unnikrishnan, Shuguang Ma, K. Vidyasagar, M. P. Antony, G. P. Selvam, V. Visalakshi, N. Chandrakumar, K. Pandian, Y-T Tao, and T. Pradeep, *Chem. Mater.* **12**, 104 (2000).
- ¹⁸N. Sandhyarani and T. Pradeep, *Chem. Mater.* **12**, 1755 (2000).
- ¹⁹S. Link, Z. L. Wang, and M. A. El-Sayed, *J. Phys. Chem. B* **103**, 3529 (1999).
- ²⁰J. Sinzig, U. Radtke, M. Quinten, and U. Kreibig, *Z. Phys. D* **26**, 242 (1993).
- ²¹M. Sheik-Bahae, A. A. Said, T. H. Wei, D. J. Hagan, and E. W. Van Stryland, *IEEE J. Quantum Electron.* **26**, 760 (1990).
- ²²S. Couris, E. Coudomas, F. Dong, and S. Leach, *J. Phys. B* **29**, 5033 (1996).
- ²³Ya-Ping Sun, J. E. Riggs, H. W. Rollins, and R. Guduru, *J. Phys. Chem. B* **103**, 77 (1999).
- ²⁴G. Mie, *Ann. Phys. (Leipzig)* **25**, 377 (1908).
- ²⁵T. S. Ahmadi, S. L. Logunov, and M. A. El-Sayed, *J. Phys. Chem.* **100**, 8053 (1996).
- ²⁶P. V. Kamat, M. Flumiani, and G. V. Hartland, *J. Phys. Chem. B* **102**, 3123 (1998).
- ²⁷S. Link, C. Burda, Z. L. Wang, and M. A. El-Sayed, *J. Chem. Phys.* **111**, 1255 (1999).
- ²⁸E. J. Heilweil and R. M. Hochstrasser, *J. Chem. Phys.* **82**, 4762 (1985).
- ²⁹T. W. Roberti, B. A. Smith, and J. Z. Zhang, *J. Chem. Phys.* **102**, 3860 (1995).
- ³⁰W. S. Fann, R. Storz, H. W. K. Tom, and J. Boker, *Phys. Rev. Lett.* **68**, 2834 (1992).
- ³¹S. D. Brorson, A. Kazeroonian, J. S. Moodera, D. W. Face, T. K. Cheng, E. P. Ippen, M. S. Dresselhaus, and G. Dresselhaus, *Phys. Rev. Lett.* **64**, 2172 (1990).
- ³²R. W. Schoenlein, W. Z. Lin, J. G. Fujimoto, and G. L. Eesley, *Phys. Rev. Lett.* **58**, 1680 (1987).
- ³³A. Ulman, *An Introduction to Ultrathin Organic Films: from Langmuir Blodgett to Self Assembly* (Academic, New York, 1991); A. Ulman, *Chem. Rev.* **96**, 1533 (1996).
- ³⁴M. R. V. Sahyun, S. E. Hill, N. Serpone, R. Danesh, and D. K. Sharma, *J. Appl. Phys.* **79**, 8030 (1996).
- ³⁵P. P. Sorokin, J. J. Luzzi, J. R. Lankard, and G. D. Pettit, *IBM J. Res. Dev.* **8**, 182 (1964).
- ³⁶L. W. Tutt and T. F. Boggess, *Prog. Quantum Electron.* **17**, 299 (1993).
- ³⁷S. Hughes and B. Wherret, *Phys. Rev. A* **54**, 3546 (1996).
- ³⁸X. Deng, X. Zhang, Y. Wang, Y. Song, S. Liu, and C. Li, *Opt. Commun.* **168**, 207 (1999).
- ³⁹S. Hughes, G. Spruce, B. S. Wherret, K. R. Whelford, and A. D. Lloyd, *Opt. Commun.* **100**, 113 (1993).
- ⁴⁰Y. B. Band, D. J. Harter, and R. Bavli, *Chem. Phys. Lett.* **126**, 280 (1986).
- ⁴¹M. J. Hostetler, C. J. Zhong, B. K. H. Yen, J. Anderegg, S. M. Gross, N. D. Evans, M. Porter, and R. W. Murray, *J. Am. Chem. Soc.* **120**, 9396 (1998).
- ⁴²H. Remita, J. Khatouri, M. Treguer, J. Amblard, and J. Belloni, *Z. Phys. D: At., Mol. Clusters* **40**, 127 (1997).
- ⁴³M. Y. Han, W. Huang, C. H. Chew, L. M. Gan, X. J. Zhang, and W. Ji, *J. Phys. Chem. B* **102**, 1884 (1998).
- ⁴⁴Results presented at the Second International Symposium on Optical Power Limiting (ISOPL-2000), held at Venice, Italy during 2nd July to 5th July 2000. Proceedings of the symposium will be forthcoming as a special issue of *Nonlinear Optics*.